ELSEVIER

Chemical Engineering Journal 142 (2008) 182–189

Chemical Engineering Journal

www.elsevier.com/locate/cej

Dispersion analysis of an acidogenic UASB reactor

Ting-Ting Ren [a], Yang Mu [a], Han-Qing Yu [a,*], Hideki Harada [b], Yu-You Li [b]

[a] *School of Chemistry, University of Science & Technology of China, School of Chemistry, 96 Jinzhai Road, Hefei 230026, China*
[b] *Department of Civil Engineering, Tohoku University, Sendai 980-8579, Japan*

Received 9 May 2007; received in revised form 7 November 2007; accepted 20 November 2007

Abstract

The dispersion behavior of an upflow anaerobic sludge blanket (UASB) reactor for acidogenesis was investigated, and its flow patterns were simulated. Compared with the single-zone axial-dispersion model (with squared difference from 130 to 450), a two-zone axial-dispersion model (with squared difference from 1 to 7) was found to be more appropriate for simulating the dispersion characteristics of the acidogenic UASB reactor. A sensitivity analysis of the key model parameters was performed, and the axial dispersion coefficient was identified as the most important factor in the dispersion modeling of the reactor, implying that the acidogenic UASB reactor was potentially dispersion-controlled. The flow patterns, including mixed and plugging degrees, at different hydraulic loading rates were evaluated. The ratio of plug volume to mixed volume (I_p/I_m) decreased with the increasing specific gas velocity (U_g^{sp}) when the U_g^{sp} value was low, but increased markedly with the increasing U_g^{sp} after the U_g^{sp} exceeded 0.7.

Keywords: Acidogenesis; Dispersion; Hydrodynamics; Model; Upflow anaerobic sludge blanket (UASB)

1. Introduction

In conventional single-phase anaerobic reactors, over production of volatile fatty acids (VFA), often attributed to loading shocks and/or other sudden changes of process conditions, could result in the lowering of pH. As a consequence, reactors would turn "sour" and cease to produce methane [1,2]. This operational problem has led to the development of the two-phase anaerobic process [3], in which acidogenesis and methanogenesis are conducted in two reactors in sequence. Despite of increased total reactor volume, the two-phase anaerobic process offers a number of advantages, e.g., easier to control and less sensitive to shocks [4]. The overall efficiency could be enhanced by operating reactors at optimal conditions respectively for acidogenesis and methanogenesis [5,6].

In biological wastewater treatment, the dispersion behavior determines the resultant mass transport processes and accordingly the final performance of a given reactor. As a multiphase anaerobic reactor, the overall dispersion behavior of an upflow anaerobic sludge blanket (UASB) reactor is the result of interactions between several interdependent physical phenomena, especial fluid flow properties, particle segregation and chaotic advection [7]. Various models have been established to describing the hydrodynamics of methanogenic reactors [8–12]. In most cases, a methane-producing UASB reactor has been modeled with an axial-dispersion model that consists of one or two compartments [13]. The axial dispersion coefficient distribution along a UASB reactor height has been described using a two-zone axial-dispersion (TZAD) model [14]. With a combination of biochemical reaction models with the hydrodynamic models, integrated mathematic models have been developed to describe the overall performance of methane-producing UASB reactors [15,16]. However, so far the flow pattern and dispersion characteristics of an acidogenic UASB reactor have not been well documented yet.

In a previous study at our laboratory, an acidogenic UASB reactor has been used to acidify sucrose-rich wastewater to produce VFA and hydrogen for over 5 years, and granules have been cultivated in this UASB reactor [17]. The physicochemical characteristics of the acidogenic granules and the long-term performance of the acidogenic granule-based UASB reactor have been reported [17,18]. The main objective of this work was to elucidate the dispersion characteristics of such an acidogenic UASB reactor. For this purpose, the mixed and plugging degrees at different hydraulic loading rates were evaluated. In addition, the TZAD model, which was developed from a single-zone

* Corresponding author. Tel.: +86 551 3607592; fax: +86 551 3601592.
E-mail address: hqyu@ustc.edu.cn (H.-Q. Yu).

1385-8947/$ – see front matter © 2007 Elsevier B.V. All rights reserved.
doi:10.1016/j.cej.2007.11.028

Nomenclature

C	tracer concentration (mg L^{-1})
$C(p)$	calculated value of the model variable (mg L^{-1})
C_a	tracer concentration at the point preceding Zone-1 of the two-zone axial-dispersion model (mg L^{-1})
C_s	concentration at the point preceding Zone-2 of the two-zone axial-dispersion model (mg L^{-1})
D	dispersion coefficient (m^2 h^{-1})
H_1	height of sludge bed (m)
H_2	height of blanket (m)
I	volume fraction
I_{in}	tracer loadings into the compartment (mg h^{-1})
N_{time}	all sampling times
p	model evaluated parameters
Q_{in}	discharge of water into the compartment (m^3 h^{-1})
S	bypass rate
t	time (h)
$\bar{t}$	mean of the residence time distribution (h)
t^*	theoretical residence time of whole reactor (h)
u	upflow velocity (m h^{-1})
U_g^{sp}	specific gas velocity
V	volume (L)
y	solution of the model equations for a given variable at a given location and time
z	axial position (m)

Greek letters

β	retention time factor
δ	element of sensitivity function
$\delta_{y,p}^{err}$	error contribution of each parameter (mg L^{-1})
θ_{peak}	dimensionless time to concentration peak
$\bar{\theta}$	mean of the dimensionless residence time distribution
σ	standard deviation (mg L^{-1})
σ_p	standard deviations of the uncertain model parameters
σ_y	approximate standard deviation of the model result
χ^2	squared difference between measured and calculated values of tracer concentrations at the sampling ports over all sampling times

Subscripts

1z	quantities in Zone-1 of the two-zone axial-dispersion model
2z	quantities in Zone-2 of the two-zone axial-dispersion model
d	dead region
g	gas
i	ith element of function
l	liquid
m	mixing-flow
n	quantities of the single-zone axial-dispersion model
p	plug-flow

Superscript

cal	calculated value
exp	measured value

axial-dispersion (SZAD) model proposed by Singhal et al. [13], was used to describe the reactor dispersion characteristics.

2. Materials and methods

2.1. Experimental setup

Experiments were carried out in a 7.5 L Plexiglas UASB reactor with an internal diameter of 10 cm and a height of 88 cm. The reactor working volume was 4.0 L. The temperature of the reactor was maintained at 37 ± 1 °C using a ribbon heater and a temperature controller.

The reactor was seeded with methanogenic sludge taken from a full-scale anaerobic reactor treating citrate-producing wastewater. The pH and volatile suspended solids (VSS) of the seed sludge were 7.1 and 6.3 g L^{-1}, respectively. The UASB reactor was inoculated with sludge of 20.0 g-VSS L^{-1}. This reactor was then shifted from a methanogenic reactor to an acidogenic one by gradually lowering the influent pH as described previously [17]. A sucrose-rich synthetic wastewater was used as substrate and was supplemented with buffering chemicals and a sufficient amount of inorganic nutrients as follows (in mg L^{-1}): NH_4HCO_3 405; $K_2HPO_4 \cdot 3H_2O$ 155; $CaCl_2$ 50; $MgCl_2 \cdot 6H_2O$ 100; $FeCl_2$ 25; NaCl 10; $CoCl_2 \cdot 6H_2O$ 5; $MnCl_2 \cdot 4H_2O$ 5; $AlCl_3$ 2.5; $(NH_4)_6Mo_7O_{24}$ 15; H_3BO_3 5; $NiCl_2 \cdot 6H_2O$ 5; $CuCl_2 \cdot 5H_2O$ 5; $ZnCl_2$ 5 [19]. The reactor effluent pH was maintained at 4.4 ± 0.1 by controlling the dosage of $NaHCO_3$. The start-up and steady-state performance of this acidogenic UASB has been reported previously [18].

The pulse–response technique was used in this study. In operation, a pulse injection of tracer Li^+ was performed at time $t = 0$ in the input stream of the reactor, and the tracer concentration at time series was measured at the outlet, which was 88 cm high from the bottom. Since the heights of sludge bed changed under varying hydraulic conditions, the measurement of tracer concentration at the bottom of sludge bed could not be achieved readily and accurately. Thus, the height of sludge bed was taken into account in experiments and calculation. A solution containing 594 mg Li_2SO_4 (75 mg Li^+) was applied in every tracer run, producing a mean Li^+ concentration in the reactor of 10 mg L^{-1}. Experiments were carried out at four hydraulic retention times (HRTs) of 4.3, 8.0, 16.3 and 26.4 h, while the corresponding heights of sludge bed were 57, 55, 52 and 50 cm, respectively (Table 1). The organic loading rate (OLR) and gas production rate at each HRT are also given in Table 1. Samples were taken every 2 and 1 h for the HRT of 26.4 and 16.3 h, respectively, and every 0.5 h for the HRT of 8.0 and 4.3 h, respectively. A peristaltic pump (BT00-100M, Longer Co.) was used to control the flow rate. Composite samples of the reactor effluent were taken in each tracer test and analyzed for Li^+ concentration.

Table 1
Experimental conditions

HRT (h)	Flow rate ($L\,h^{-1}$)	OLR (g-COD $L^{-1}\,d^{-1}$)	Gas production rate (mL $L^{-1}\,h^{-1}$)	H_1[a] (cm)	H_2[b] (cm)
26.4	0.150	9.0	60.6 ± 3.0	50	38
16.3	0.245	14.7	64.4 ± 3.2	51	37
8.0	0.500	30.0	283.3 ± 14.1	52	36
4.3	0.930	55.8	436.7 ± 21.4	57	31

[a] Height of sludge bed.
[b] Height of blanket.

2.2. Analysis

Lithium concentration was determined using flame emission spectroscopy (Vario 6, Analytik Jena AG) at a wavelength over 670.8 nm, slit width of 0.5 nm, and a plus of air-acetylene. Series dilutions of five standards were prepared and triplicates were injected for calibration. Samples concentrations were calculated based on the standard curve according to the standard methods [20].

The concentrations of ethanol and VFA, including acetate, propionate, butyrate, *i*-butyrate, valerate and caproate, in the effluent were determined with gas chromatograph (6890NT, Agilent Inc.) equipped with a flame ionization detector and a $30\,m \times 0.25\,mm \times 0.25\,\mu m$ fused-silica capillary column (DB-FFAP). Sucrose concentration was determined by using anthrone-sulfuric acid method [21].

With the data of transient tracer concentrations at the outlet of the reactor, the value of parameters t^*,$\bar{t}$, and $\bar{\theta}$ of retention time distribution (RTD) experiments could be calculated with the formulas described by Martin [22]. In addition, a number of additional empirical parameters, such as retention time factor (β), fraction of plug volume (I_p), dead volume (I_d) and mixed volume (I_m), were defined to characterize the hydrodynamics of a bioreactor [7,22] as following:

$$\beta = \frac{\bar{t}}{t^*} \tag{1}$$

$$I_p = \frac{V_p}{V} = \frac{\theta_{peak}}{\bar{\theta}} \tag{2}$$

$$I_d = \frac{V_d}{V} = 1 - \frac{\bar{t}}{t^*} = 1 - \beta \tag{3}$$

$$I_m = \frac{V_m}{V} = 1 - \frac{V_p}{V} - \frac{V_d}{V} \tag{4}$$

3. Model description

3.1. SZAD model

In the SZAD model, the physical and microbiological processes inside the reactor were considered to be dependent only on the vertical axis of the reactor (distance z from input, z varied from 0 to H) and time t, i.e., all the process characteristics in fixed cross-section were uniform [15]. In general, the phenomenon of axial dispersion could be described by a differential equation in the SZAD model according to Brenner [23]:

$$\frac{\partial C}{\partial t} = D_n \frac{\partial^2 C}{\partial z^2} - u \frac{\partial C}{\partial z} \tag{5}$$

3.2. TZAD model

In the TZAD model the sludge bed was considered as Zone-1 and the liquid above the bed as Zone-2 [13]. The existence of liquid bypass [13] was assumed for Zone-1, while stagnant regions were neglected.

The mass balance for the tracer in Zone-1 was given in Eq. (6) with Danckwerts [24] boundary conditions in Eqs. (7) and (8):

$$\frac{\partial C_{1z}}{\partial t} = D_{1z} \frac{\partial^2 C_{1z}}{\partial^2 z_{1z}} - u_{1z} \frac{\partial C_{1z}}{\partial z_{1z}} \tag{6}$$

$$\text{B.C.}: \quad D_{1z} \frac{\partial C_{1z}}{\partial z_{1z}} = u_{1z}(C_{1z} - C_a) \quad z_{1z} = 0 \tag{7}$$

$$\frac{\partial C_{1z}}{\partial z_{1z}} = 0 \quad z_{1z} = H_1 \tag{8}$$

Similarly, the mass balance in the Zone-2 was written as Eq. (9) with the boundary conditions given in Eqs. (10) and (11).

$$\frac{\partial C_{2z}}{\partial t} = D_{2z} \frac{\partial^2 C_{2z}}{\partial^2 z_{2z}} - u_{2z} \frac{\partial C_{2z}}{\partial z_{2z}} \tag{9}$$

$$\text{B.C.}: \quad D_{2z} \frac{\partial C_{2z}}{\partial z_{2z}} = u_{2z}(C_{2z} - C_s) \quad z_{2z} = 0 \tag{10}$$

$$\frac{\partial C_{1z}}{\partial z_{2z}} = 0 \quad z_{2z} = H_2 \tag{11}$$

The water and tracer loadings at the point proceeding of Zone-1 and Zone-2 were respectively described in Eqs. (12) and (13):

$$I_{in,1z} = Q_{in} C_a (1 - S) \tag{12}$$

$$I_{in,2z} = Q_{in} C_s (1 - S) + Q_{in} S C_a \tag{13}$$

3.3. Sensitivity

In the TZAD model, since the parameters D_{z1}, D_{z2} and S were not correlated with each other, a sensitivity analysis was then performed to examine the significance of each model parameter. The absolute-relative sensitivity function was employed to evaluate the ratio of the changes in the calculated effluent tracer

Table 2
Substrate degradation and distribution of VFA and ethanol in the reactor effluent at various HRTs

HRT (h)	VFA (mg L^{-1})						Ethanol (mg L^{-1})	Substrate removal efficiency (%)
	Acetate	Propionate	Butyrate	*i*-Butyrate	Valerate	Caproate		
26.4	660.40 ± 23.25	324.36 ± 16.22	15.63 ± 4.23	1754.65 ± 46.52	394.70 ± 15.32	2.00 ± 0.09	17.30 ± 0.85	99.5 ± 0.20
16.3	501.71 ± 24.32	359.25 ± 17.96	9.29 ± 0.45	1452.49 ± 23.78	374.74 ± 13.20	1.50 ± 0.11	10.80 ± 0.25	99.5 ± 0.30
8.0	778.11 ± 38.56	512.85 ± 25.61	13.26 ± 0.66	1666.75 ± 38.35	636.64 ± 28.56	0.40 ± 0.01	17.70 ± 0.59	97.6 ± 0.54
4.3	401.76 ± 20.05	157.92 ± 7.85	6.97 ± 0.24	1191.34 ± 29.86	308.87 ± 12.56	4.10 ± 0.12	6.80 ± 0.37	96.1 ± 0.89

concentration $C_i^{cal}(p)$ to those in the parameter values p_i with the following equation:

$$\delta_i = p_i \frac{\partial C_i^{cal}(p)}{\partial p} \tag{14}$$

This equation could be used to evaluate the absolute change in $C_i^{cal}(p)$ for a 100% change in p_i.

In addition, the uncertainty of model parameters was propagated to the uncertainty of model results. Eq. (15) gave the error propagation formula using a linearized form:

$$\sigma_y = \sqrt{\sum_{t=1}^{m} \left(\frac{\partial y}{\partial p_i}\right)^2 \sigma_{p_i}^2} \tag{15}$$

The error contribution of each parameter was calculated as following:

$$\delta_{y,p}^{err} = \frac{\partial y}{\partial p}\sigma_p \tag{16}$$

3.4. Parameter estimation

The parameters in axial-dispersion model were estimated by minimizing the sum of the squared difference χ^2 between measured (C^{exp}) and calculated (C^{cal}) values of tracer concentrations at the sampling ports over all sampling times (N_{time}), i.e., the following function was minimized in the following equation:

$$\chi^2 = \sum_{i=1}^{N_{time}} \left(\frac{C_i^{cal}(p) - C_i^{exp}}{\sigma_i^{exp}}\right)^2 \tag{17}$$

Software AQUASIM 2.0 [25] was used for the calculation and parameter estimation. The parameter estimation and parameter uncertainty evaluation were achieved with a 95% confidence level for significance testing and parameter uncertainty analysis.

4. Results

4.1. Flow patterns

Comparative performance of the acidogenic UASB reactor at various HRTs is summarized in Table 2. VFA and ethanol are the main aqueous products for acidogenesis process. Butyrate was of a high level and even became dominant. As shown in Table 2, the total VFA and ethanol concentration significantly changed as the HRT was altered.

The hydrodynamic parameters obtained at the reactor outlet, including retention time factor (β), fraction of plug volume (I_p), dead volume (I_d) and mixed volume (I_m), are summarized in Table 3. The smaller β values for an HRT of 8.0 h indicate a dead zone for this run. This is confirmed by the lower tracer recoveries shown in Table 3.

The ratio of plug volume to mixed volume, defined as I_p/I_m, is regarded as the fluid dynamic parameter to indicate the level of plugging in the reactor. Since biogas bubbles and liquid simultaneously transport through the sludge bed and blanket, an index, specific gas velocity U_g^{sp}, is introduced to separately evaluate the effect of the biogas bubble transport on the flow pattern:

$$U_g^{sp} = \frac{u_g}{u_g + u_l} \tag{18}$$

The relationship between I_p/I_m and U_g^{sp} in Fig. 1 shows that I_p/I_m decreased with the increasing U_g^{sp} when the U_g^{sp} value was low, but increased with the increasing U_g^{sp} after the U_g^{sp} exceeded 0.7.

Mixing in a multiple-phase continuously flow reactor such as a UASB is dependent mainly on liquid velocity, gas velocity, phase (gas, liquid, and solid) physical properties, phase hold-up, and reactor geometry. None of these factors is isolated to discriminate their effects on mixing in a UASB reactor, as gas velocity, liquid velocity and phase hold-up change simultaneously and their effects overlap with each other in the experiments. Phase physical properties, phase hold-up and reac-

Table 3
Hydrodynamic characteristics of the acidogenic UASB reactor

HRT (h)	β	Li$^+$ (%)	θ_{peak}	u_g (m h^{-1})	u_l (m h^{-1})	I_p	I_d	I_m
4.3	0.93	99.60	0.48	0.411	0.118	0.45	0.07	0.48
8.0	0.83	97.50	0.53	0.271	0.064	0.44	0.17	0.39
16.3	1.03	99.85	0.39	0.059	0.031	0.40	0.00	0.60
26.4	0.98	99.60	0.37	0.049	0.019	0.36	0.02	0.62

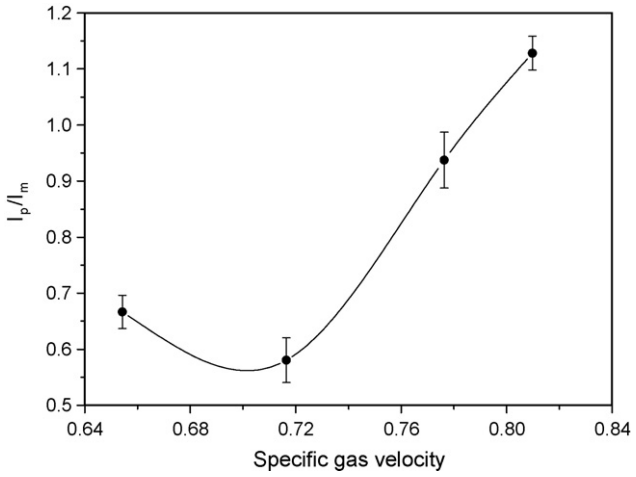

Fig. 1. Relationships between the ratios of plug to mixed volume (I_p/I_m) and specific gas velocity. HRT for the four points (left to right) were 16.3, 26.4, 4.3 and 8.0 h.

tor geometry are different for various systems or operating under varying loading conditions, and accordingly they lack of generality. However, the specific gas velocity, which is the result of these properties, would be an appropriate parameter to assess the mixing in a bioreactor.

4.2. Sensitivity analysis

The absolute-relative sensitivity values of the three parameters (∂S, ∂D_{z1} and ∂D_{z2}) calculated from Eq. (14) are shown in Fig. 2. Compared with ∂S, ∂D_{z1} and ∂D_{z2} resulted in a more pronounced change in the effluent tracer concentration.

The error contributions of the three parameters are shown in Fig. 3. The sensitivity analysis results suggest that the dispersion coefficient had the most influence on the outcome of parameter estimation. Thus, the dispersion coefficient needs a further study to improve the model prediction. Although the effect of S value is not significant, bypass was also estimated from a model exactitude point of view [13].

4.3. Model simulation and comparison

Parameter estimation was achieved and the resulting parameters of TZAD model are given in Table 4. For the parameter estimation of the TZAD model, there was a good agreement between the measured and calculated tracer trajectories, as shown in Fig. 4. The TZAD model was effective in simulating the acidogenic UASB. On the other hand, the SZAD model was inadequate for describing the dispersion behaviors of such a reactor, as shown in Table 4 and Fig. 4. It demonstrated that the non-uniform dispersion was the crucial characteristics in the acidogenic UASB reactor.

Table 4
Estimation parameters of the axial-dispersion models

Model	Parameter	HRT (h)			
		4.3	8.0	16.3	26.4
TZAD model	D_{1z} ($m^2\,h^{-1}$)	0.180	0.122	0.114	0.100
	D_{2z} ($m^2\,h^{-1}$)	0.010	0.003	0.006	0.004
	S	0.001	0.059	0.000	0.000
	Final χ^2	1	4	6	7
SZAD model	D_n ($m^2\,h^{-1}$)	0.046	0.020	0.014	0.01
	Final χ^2	186	448	321	136

5. Discussion

5.1. Degree of plug-flow

Plug-flow has advantages over other flow patterns from a substrate removal point of view, because there is a high driving force for substrate removal at the inlet of reactor [9]. Thus, the plug-flow degree in the acidogenic UASB reactor should be evaluated. Gas flow rate, especially in the bubble flow regime, and upflow liquid velocity ($u_l < 30\,m\,h^{-1}$), affected the liquor mixing intensity [26], which in turn influenced the degree of plug-flow. In the UASB reactor the gas flow had a significant impact on the degree of plug-flow, as shown in Fig. 1. Because of a low upflow liquid velocity, the biogas production rate had a much more important effect on the flow patterns of the acidogenic UASB reactor [12]. When the specific gas velocity value reached a certain value (approximately 0.7 in this work), the biogas production rates became the main factor governing the reactor hydrodynamic behavior (Fig. 1). Biogas production might also be one reason for bypass flow at a high hydraulic loading rate, which corresponded to a high organic load rate [27]. A high gas production rate brought on the bobble coalescent, which caused channeling and induced bypass in the reactor.

5.2. Evaluation of the TZAD model

This study demonstrates that the TZAD model was appropriate for simulating the dispersion behavior of the acidogenic UASB reactor (Fig. 4). In the TZAD model, the dispersion change along the UASB reactor was considered, and the different dispersion coefficients in sludge bed and sludge blanket were taken into account. There are several reasons responsible for the different dispersion coefficients for the sludge bed and blanket regions. The size distribution and granules filling gradient was an important factor, which would result in a higher apparent linear upflow velocity and tighter packing in the bottom of sludge bed than at the bed top or in the liquid zone. Other significant axial gradients, such as substrate, VFA and pH, were also important factors. The presence of bacteria excreta, fine solids and colloidal materials might also be responsible for such a difference [28], which results in the viscosity variation of liquid throughout reactor.

5.3. Dispersion features of an acidogenic reactor

The physicochemical characteristics of the acidogenic granules were found to be different from those of the methanogenic granules in some aspects. For instance, the porosity of the former was much less than that of the latter [17,29]. The total extracellular polymeric substances (EPS) content in the former

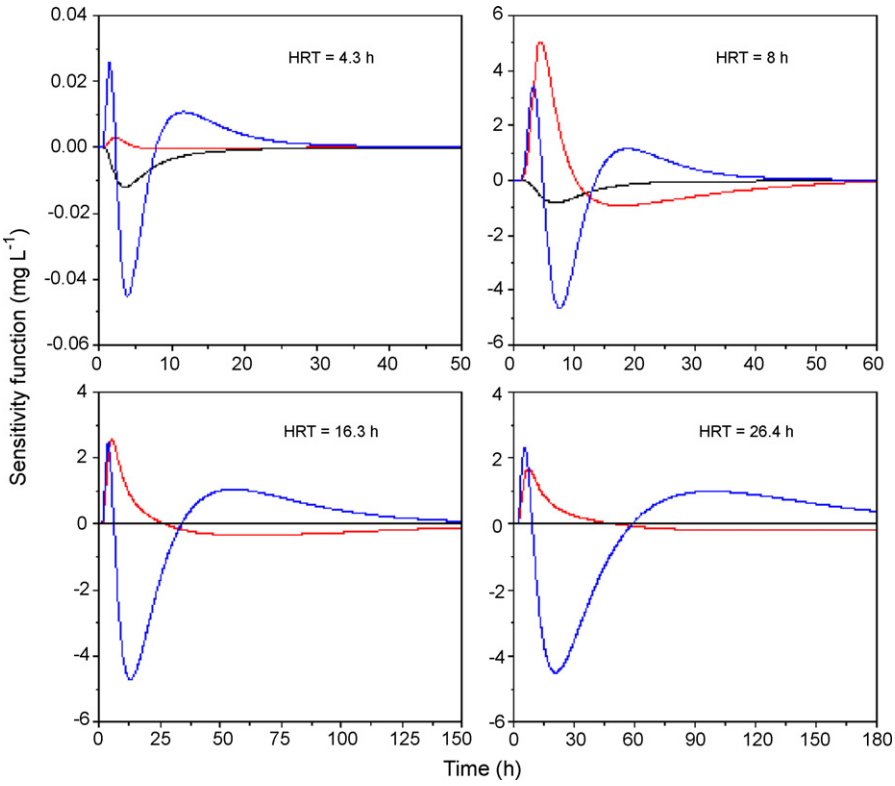

Fig. 2. Sensitivity function of a calculated Li^+ concentration with respect to the three model parameters ((– – –, red in the web version) D_1; (– – –, blue in the web version) D_2; (– – –) S) at various HRTs.

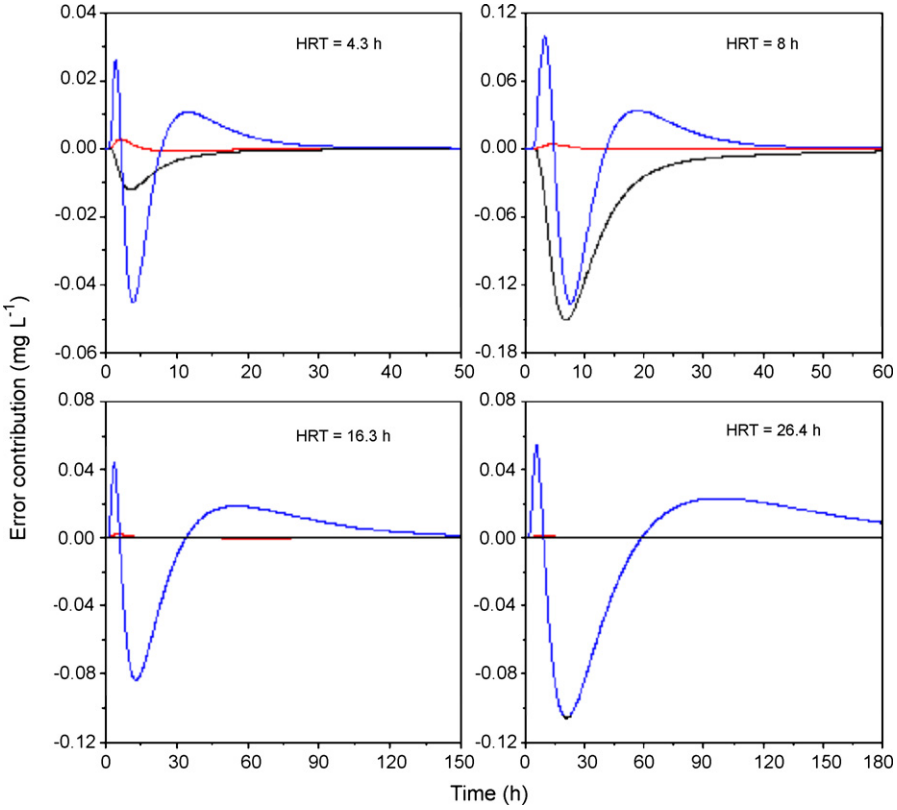

Fig. 3. Error contribution of the three parameters ((– – –, red in the web version) D_1; (– – –, blue in the web version) D_2; (– – –) S) to a calculated Li^+ concentration at various HRTs.

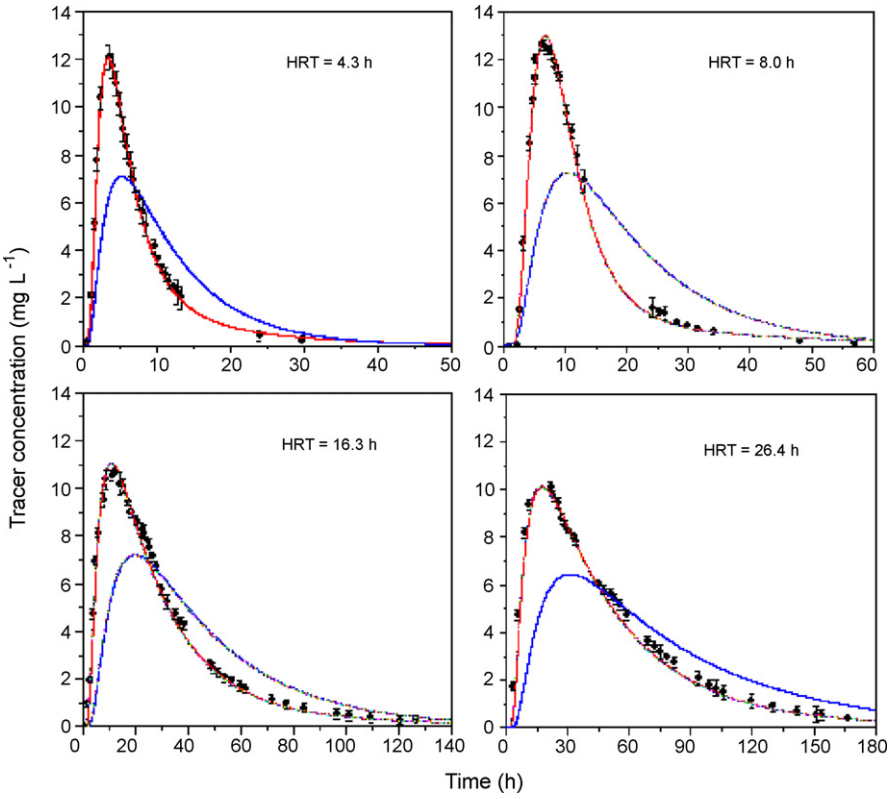

Fig. 4. Comparison of the simulated (TZAD model: red lines; SZAD model: blue lines) and experimental (dotted lines) tracer concentrations in the effluent at various HRTs. (For interpretation of the references to color in this figure legend, the reader is referred to the web version of the article.)

was substantially higher than the latter [17]. As a consequence, the lower permeabilities of the acidogenic granules result in less advective flow through their interior than those of the methanogenic ones [17,29]. Although these differences may not result in a significant difference in reactor hydraulic behaviors, a lower porosity and permeability of the acidogenic granules should have contributed to the dispersion features of an acidogenic UASB reactor compared with a methanogenic one. Granular sludge is the key element in both acidogenic and methanogenic UASB reactors, and its physicochemical characteristics have an effect on the dispersion behavior of UASB reactors [12,28].

Another significant dispersion feature of an acidogenic UASB reactor is related with gas production rate. For two identical lab-scale UASB reactors seeded with the same level of sucrose-rich wastewater, the gas production rate in an acidogenic UASB reactor was one-third less than that in a methanogenic one [18]. A lower gas producing rate would lead to the distinguishing dispersion feature of this UASB reactor [14]. The liquid viscosity increased after acidogenesis of substrate [17], which also should have a contribution to the dispersion feature of an acidogenic UASB reactor [28].

It should be mentioned that only the hydrodynamics of a laboratory-scale acidogenic UASB reactor was modeled in this work. The hydrodynamics of a full-scale acidogenic reactor could be completely different in terms of liquid upflow velocity, accumulating gas upflow velocity and sudden release of enclosed biogas bubbles in the sludge bed. Therefore, it should be cautious to apply these models to simulate or predict the hydrodynamic behaviors of full-scale acidogenic UASB reactors. However, since both substrate degradation and VFA production were correlated with dispersion behavior of the reactor, dispersion analysis on an acidogenic UASB reactor would be useful.

Both reactions kinetics and dispersion have significant contributions to in properly characterizing the performance of UASB reactors. The dispersion behavior governs the resultant mass transport processes and accordingly the overall performance of the reactor. Kinetics and mass transfer factors can be added in Eqs. (6–11), and then a comprehensive model combining dispersion, mass transfer and biochemical kinetics could be established. Such a model is able to well describe the overall performance of an acidogenic UASB reactor [15]. Therefore, the dispersion model simulation and prediction can provide a solid foundation for design and operation of such acidogenic systems.

6. Conclusions

In this work the dispersion characteristics of an acidogenic UASB reactor was explored. The flow patterns, including mixed and plugging degrees, at different hydraulic loading rates were simulated to explore the axial dispersion in the UASB reactor. Compared with the single-zone axial-dispersion model, a two-zone axial-dispersion model was found to be more appropriate for simulating the dispersion characteristics of this reactor. With sensitivity analysis of the key model parameters, axial disper-

sion coefficient was identified as the key factor in the dispersion modeling. This also suggests that the acidogenic UASB reactor was potentially dispersion-controlled.

Acknowledgements

The authors wish to thank the Natural Science Foundation of China (20577048, 50625825 and 50738006), the Chinese Academy of Sciences (KSCX2-YW-G-001), and National Basic Research Program of China (2004CB719602) for the partial support of this study.

References

[1] J.J. Lay, Y.J. Lee, T. Noike, Feasibility of biological hydrogen production from organic fraction of municipal solid waste, Water Res. 33 (1999) 2579–2586.
[2] I. Hussy, F.R. Hawkes, R. Dinsdale, D.L. Hawkes, Continuous fermentative hydrogen production from a wheat starch co-product by mixed microflora, Biotechnol. Bioeng. 84 (2003) 619–626.
[3] F.G. Pohland, S. Ghosh, Developments in anaerobic stabilization of organic wastes, the two-phase concept, Environ. Technol. 1 (1971) 255–266.
[4] P. Pipyn, W. Verstraete, Lactate and ethanol as intermediates in two-phase anaerobic digestion, Biotechnol. Bioeng. 23 (1981) 1145–1154.
[5] H.H.P. Fang, H.Q. Yu, Mesophilic acidification of galetinaceous wastewater, J. Biotechnol. 93 (2002) 99–108.
[6] S.E. Oh, S. van Ginkel, B.E. Logan, The relative effectiveness of pH control and heat treatment for enhancing biohydrogen gas production, Environ. Sci. Technol. 37 (2003) 5186–5190.
[7] M.R. Pena, D.D. Mara, G.P. Avella, Dispersion and treatment performance analysis of an UASB reactor under different hydraulic loading rates, Water Res. 40 (2006) 445–452.
[8] P.M. Heertjes, R.R. van der Meer, Dynamics of liquid flow in an upflow reactor used for anaerobic treatment of wastewater, Biotechnol. Bioeng. 20 (1978) 1577–1594.
[9] P.M. Heertjes, L.J. Kuijvenhoven, Fluid flow pattern in upflow reactors for anaerobic treatment of beet sugar factory wastewater, Biotechnol. Bioeng. 24 (1982) 443–459.
[10] W.L. Bolle, J. van Breugel, G.C. van Eybergen, N.W.F. Kossen, R.J. Zoetemeyer, Modeling the liquid flow in p-flow anaerobic sludge blanket reactor, Biotechnol. Bioeng. 28 (1986) 1615–1620.
[11] S.K. Narnoli, I. Mehrotra, Sludge blanket of UASB reactor: mathematical simulation, Water Res. 31 (1997) 715–726.
[12] S. Kalyuzhnyi, V. Fedorovich, P. Lens, Dispersed plug flow model for UASB reactors focusing on sludge dynamics, J. Ind. Microbiol. Biotechnol. 33 (2006) 221–237.
[13] A. Singhal, J. Gomes, V.V. Praveen, K.B. Ramachandran, Axial dispersion model for upflow anaerobic sludge blanket reactors, Biotechnol. Prog. 14 (1998) 645–648.
[14] Y. Zeng, S.J. Mu, S.J. Lou, B. Tartakovsky, S.R. Guiot, P. Wu, Hydraulic modeling and axial dispersion analysis of UASB reactor, Biochem. Eng. J. 25 (2005) 113–123.
[15] S. Kalyuzhnyi, V. Fedorovich, Integrated mathematical model of UASB reactor for competition between sulphate reduction and methanogenesis, Water Sci. Technol. 36 (1997) 201–208.
[16] S. Kalyuzhnyi, V. Fedorovich, P. Lens, L.H. Pol, G. Lettinga, Mathematical modelling as a tool to study population dynamics between sulfate reducing and methanogenic bacteria, Biodegradation 9 (1998) 187–199.
[17] Y. Mu, H.Q. Yu, Biological hydrogen production in a UASB reactor with granules I: physicochemical characteristics of hydrogen-producing granules, Biotechnol. Bioeng. 94 (2006) 980–985.
[18] H.Q. Yu, Y. Mu, Biological hydrogen production in a UASB reactor with granules II: reactor performance in 3-year operation, Biotechnol. Bioeng. 94 (2006) 988–995.
[19] S.E. Oh, P. Iyer, M.A. Bruns, B.E. Logan, Biological hydrogen production using a membrane bioreactor, Biotechnol. Bioeng. 87 (2004) 119–127.
[20] APHA, Standard Methods for the Examination of Water and Wastewater, 19th ed., American Public Health Association, Washington, DC, 1995.
[21] M. Dubois, K.A. Gilles, J.K. Hamilton, P.A. Rebers, F. Smith, Colorimetric method for determination sugars and related substance, Anal. Chem. 28 (1956) 350–356.
[22] A.D. Martin, Interpretation of residence time distribution data, Chem. Eng. Sci. 55 (2000) 5907–5917.
[23] H. Brenner, The diffusion model of longitudinal mixing in beds of finite length, Chem. Eng. Sci. 17 (1962) 229–237.
[24] P.V. Danckwerts, Continuous flow systems—distribution of residence times, Chem. Eng. Sci. 2 (1953) 1–13.
[25] P. Reichert, AQUASIM—a tool for simulation and data analysis of aquatic systems, Water Sci. Technol. 30 (1994) 21–30.
[26] I. Iliuta, F.C. Thyrion, O. Muntean, Axial dispersion of liquid in gas-liquid co-current downflow and upflow fixed-bed reactors with porous particles, Trans. Chem. Eng. 76 (1998) 64–72.
[27] D.J. Batstone, J.L.A. Hernandez, J.E. Schmidt, Hydraulics of laboratory and full-scale upflow anaerobic sludge blanket (UASB) reactors, Biotechnol. Bioeng. 91 (2005) 387–391.
[28] E.C. Pires, W.S. Hanisch, M.A.N. Andrade, An original procedure for physical simulation of upflow anaerobic sludge blanket reactors, Bioprocess Eng. 23 (2000) 389–395.
[29] Y. Mu, H.Q. Yu, G. Wang, Permeabilities of anaerobic CH_4-producing granules, Water Res. 40 (2006) 1811–1815.